Human Apolipoprotein A-I Gene Transfer Reduces the Development of Experimental Diabetic Cardiomyopathy

Sophie Van Linthout, Frank Spillmann, Alexander Riad, Christiane Trimpert, Joke Lievens, Marco Meloni, Felicitas Escher, Elena Filenberg, Okan Demir, Jun Li, Mehdi Shakibaei, Ingolf Schimke, Alexander Staudt, Stephan B. Felix, Heinz-Peter Schultheiss, Bart De Geest and Carsten Tschöpe

Circulation 2008;117;1563-1573; originally published online Mar 10, 2008;
DOI: 10.1161/CIRCULATIONAHA.107.710830
Circulation is published by the American Heart Association. 7272 Greenville Avenue, Dallas, TX 72514
 Print ISSN: 0009-7322. Online ISSN: 1524-4539

Human Apolipoprotein A-I Gene Transfer Reduces the Development of Experimental Diabetic Cardiomyopathy

Sophie Van Linthout, PhD; Frank Spillmann, MD; Alexander Riad, MD; Christiane Trimpert, MSc; Joke Lievens, PhD; Marco Meloni, BS; Felicitas Escher, MD; Elena Filenberg, MD; Okan Demir, MD; Jun Li, MD; Mehdi Shakibaei, MD; Ingolf Schimke, MD, PhD; Alexander Staudt, MD; Stephan B. Felix, MD; Heinz-Peter Schultheiss, MD; Bart De Geest, MD, PhD; Carsten Tschöpe, MD

Background—The hallmarks of diabetic cardiomyopathy are cardiac oxidative stress, intramyocardial inflammation, cardiac fibrosis, and cardiac apoptosis. Given the antioxidative, antiinflammatory, and antiapoptotic potential of high-density lipoprotein (HDL), we evaluated the hypothesis that increased HDL via gene transfer (GT) with human apolipoprotein (apo) A-I, the principal apolipoprotein of HDL, may reduce the development of diabetic cardiomyopathy.

Methods and Results—Intravenous GT with 3×10^{12} particles/kg of the E1E3E4-deleted vector *Ad.hapoA-I*, expressing human apoA-I, or *Ad.Null*, containing no expression cassette, was performed 5 days after streptozotocin (STZ) injection. Six weeks after apoA-I GT, HDL cholesterol levels were increased by 1.6-fold ($P<0.001$) compared with diabetic controls injected with the *Ad.Null* vector (STZ-*Ad.Null*). ApoA-I GT and HDL improved LV contractility in vivo and cardiomyocyte contractility ex vivo, respectively. Moreover, apoA-I GT was associated with decreased cardiac oxidative stress and reduced intramyocardial inflammation. In addition, compared with STZ-*Ad.Null* rats, cardiac fibrosis and glycogen accumulation were reduced by 1.7-fold and 3.1-fold, respectively ($P<0.05$). Caspase 3/7 activity was decreased 1.2-fold ($P<0.05$), and the ratio of Bcl-2 to Bax was upregulated 1.9-fold ($P<0.005$), translating to 2.1-fold ($P<0.05$) reduced total number of cardiomyocytes with apoptotic characteristics and 3.0-fold ($P<0.005$) reduced damaged endothelial cells compared with STZ-*Ad.*Null rats. HDL supplementation ex vivo reduced hyperglycemia-induced cardiomyocyte apoptosis by 3.4-fold ($P<0.005$). The apoA-I GT-mediated protection was associated with a 1.6-, 1.6-, and 2.4-fold induction of diabetes-downregulated phospho to Akt, endothelial nitric oxide synthase, and glycogen synthase kinase ratio, respectively ($P<0.005$).

Conclusion—ApoA-I GT reduced the development of streptozotocin-induced diabetic cardiomyopathy. **(*Circulation*. 2008;117:1563-1573.)**

Key Words: cardiomyopathy ■ diabetes mellitus ■ gene therapy

Diabetic patients have an increased risk of heart failure. Accumulated evidence indicates that this may be partially due to diabetic cardiomyopathy, a specific cardiomyopathy that occurs in the absence of coronary artery disease or systemic hypertension.[1] In type I insulin-dependent diabetes, this myocardial dysfunction has been experimentally characterized by cardiac oxidative stress, intramyocardial inflammation, interstitial and perivascular fibrosis, and myocardial apoptosis.[2–4] Several studies have demonstrated that hyperglycemia directly causes cardiac damage, contributing to the development of diabetic cardiomyopathy.[5,6] However, the pathological relevance of the different metabolic perturbations that accompany diabetes, including dyslipidemia, and the cellular consequences leading to altered myocardial structure and function remain incompletely understood.

Clinical Perspective p 1573

Several clinical studies have demonstrated that increased high-density lipoprotein cholesterol (HDL-C) is associated with a reduced incidence of ischemic cardiovascular diseases.[7,8] The protective effects of HDL in this setting have been attributed mainly to its role in transporting the excess of cholesterol from the peripheral tissues to the liver (reverse cholesterol transport). However, the effects of HDL are

Received August 16, 2006; accepted January 18, 2008.

From Abteilung für Kardiologie und Pneumologie, Charité-Universitätsklinikum Berlin, Campus Benjamin Franklin, Berlin, Germany (S.V.L., F.S., A.R., M.M., F.E., E.F., O.D., H.-P.S., C. Tschöpe); Klinik für Innere Medizin B, Ernst-Moritz-Arndt-Universität, Greifswald, Germany (C. Trimpert, A.S., S.B.F.); Center for Molecular and Vascular Biology, University of Leuven, Leuven, Belgium (J. Lievens, B.D.G.); Charité University Medicine Berlin, Campus Mitte, Center for Cardiovascular Research (J. Li) and Department of Cardiology (I.S.), Berlin, Germany; and Ludwig Maximilians University Munich, Faculty of Medicine, Institute of Anatomy, Musculoskeletal Research Group, Munich, Germany (M.S.).

Correspondence to Carsten Tschöpe, MD, Abteilung für Kardiologie und Pneumologie, Charité-Universitätsklinikum Berlin, Campus Benjamin Franklin, Hindenburgdamm 30, 12200 Berlin, Germany. E-mail carsten.tschoepe@charite.de

Circulation **is available at http://circ.ahajournals.org** **DOI: 10.1161/CIRCULATIONAHA.107.710830**

pleiotropic, including its direct antioxidative, antiinflammatory, and antiapoptotic features.[9–11] These pleiotropic effects involve the activation of the survival protein kinase B Akt,[12] which has been reported to be reduced in experimental type I diabetes.[13]

Given the known antioxidative, antiinflammatory, and antiapoptotic potential of HDL, we evaluated the hypothesis that increasing HDL via human apoA-I gene transfer (GT) prevents the development of streptozotocin-induced diabetic cardiomyopathy. ApoA-I is the main apolipoprotein of HDL, and plasma apoA-I levels are strongly correlated to plasma HDL-C levels. Our data indicate a direct cardioprotective effect of human apoA-I GT. An increase in HDL via human apoA-I GT blunted the development of streptozotocin-induced diabetic cardiomyopathy as evidenced by the reduction in cardiac oxidative stress, cardiac inflammation, cardiac fibrosis, cardiomyocyte apoptosis, and cardiac glycogen accumulation and subsequent improved left ventricular (LV) function despite severe hyperglycemia and unaltered levels of low-density lipoprotein cholesterol (LDL-C).

Methods

Animals

All animal experiments conformed to the *Guide for the Care and Use of Laboratory Animals* published by the US National Institutes of Health (NIH publication No. 85-23, revised 1996) and were approved by the Ethics Committee for the Use of Experimental Animals of the Charité of Berlin (Germany). Eight-week-old male Sprague-Dawley (SD) rats (300 to 330 g; Charles River Laboratories, Bar Harbor, Me) were maintained on a 12-hour light/dark cycle and fed a standard chow ad libitum. Diabetes mellitus was induced by a single injection of streptozotocin (70 mg/kg IP) prepared in 0.1 mol/L sodium citrate buffer (Sigma, Munich, Germany), pH 4.5, as described in detail previously.[14] Only rats with blood glucose levels ≥300 mg/dL 4 days after streptozotocin injection were included in the study. Intravenous GT was performed 5 days after streptozotocin injection in diabetic rats with 3×10^{12} particles/kg of the helper-independent E1E3E4-deleted adenoviral vector *Ad.hapoA-I* (containing the 1.5 kb human α_1-*antitrypsin* promoter upstream of the genomic human *apoA-I* sequence and 4 copies of the human *apoE* enhancer), inducing hepatocyte-specific and long-term expression,[15] or of *Ad.Null*, containing no expression cassette.[15] Age-matched nondiabetic SD rats injected with the same dose of *Ad.Null* were used as controls. Blood was withdrawn by eye bleeding at days 6, 12, 20, and 32 after GT for determination of human apoA-I concentrations and at the day of death for analysis of human apoA-I concentrations, triglycerides, total cholesterol, very LDL cholesterol (VLDL-C), intermediate-density lipoprotein cholesterol (IDL-C), LDL-C, HDL-C, and thiobarbituric acid reactive substances (TBARS) levels.

After hemodynamic characterization at the end of the experiment, the hearts were excised and separated in the LV and right ventricle. For cardiac morphology analysis, total heart, LV, and right ventricular weights were measured and normalized to body weight. The LV was sliced into 3 transverse sections: 1 was fixated for 24 hours in formalin and subsequently imbedded in paraffin; the second and third sections were rapidly frozen in liquid nitrogen and stored at −80°C for immunohistology (Tissue Teck, Nussloch, Germany) and molecular biology purposes.

Human ApoA-I ELISA

Human apoA-I levels were determined by sandwich ELISA as described previously.[16]

Plasma Lipid and Lipoprotein Analyses

Lipoproteins were separated from 300 μL plasma by density gradient ultracentrifugation essentially as described by Chapman et al.[17] Plasma density was adjusted to 1.23 g/mL with NaBr, and the volume was made up to 500 μL with NaBr 1.23 g/mL before transfer into Ultra-Clear centrifugation tubes (Beckman Coulter GmBH, Krefeld, Germany). Plasma was carefully overlayered with a density gradient of 500 μL NaBr 1.21 g/mL, 750 μL NaBr 1.063 g/mL, 750 μL NaBr 1.019 g/mL, 1000 μL NaBr 1.006 g/mL, and 1500 μL isotonic saline buffer. All NaBr solutions contained 0.05% EDTA, pH 7.0, to avoid oxidation of lipoproteins during centrifugation. After 22 hours of centrifugation at 30 500 rpm, fractions were isolated from the meniscus downward. All steps were carried out at 20°C. Subsequently, total cholesterol in every lipoprotein fraction was determined enzymatically. Precipath L (Roche Diagnostics, Basel, Switzerland) was used as a standard. After 1 hour of incubation at 37°C, the optical density was measured at 490 nm.

Hemodynamic Characterization

Rats were anesthetized with sodium pentobarbital (60 mg/kg IP), intubated, and artificially ventilated. Measures of LV contractility (dP/dtmax) and relaxation (dP/dtmin) were obtained with a Millar 2.0F-tip catheter (Millar Instruments Inc, Houston, Tex) as described in detail elsewhere.[3,4]

Isolation of Rat Cardiomyocytes

Hearts of male adult SD rats (anesthetized with trapanal 375 mg/kg IP) were excised, mounted on a Langendorff apparatus, and perfused with modified Krebs-Henseleit buffer containing 110 mmol/L NaCl, 2.6 mmol/L KCl, 1.2 mmol/L $MgSO_4$, 1.2 mmol/L KH_2PO_4, 11 mmol/L glucose, and 25 mmol/L HEPES, pH=7.4. For digestion, collagenase type II (Worthington, Lakewood, NJ) and 33 mmol/L $CaCl_2$ were added. Perfusion took 25 minutes with a constant pressure of 65 mm Hg. The media were maintained at 37°C and saturated with oxygen. Ventricles were minced in the same buffer, dispersed for another 10 minutes, and filtered through a mesh (200 μm) to remove undigested tissue. The isolated cardiomyocytes were washed twice with enzyme-free buffer and underwent a stepwise increase of Ca^{2+} concentration (200 and 500 μmol/L). Finally, the cell suspension was resuspended in a buffer containing 117 mmol/L NaCl, 2.8 mmol/L KCl, 0.6 mmol/L $MgCl_2$, 1.2 mmol/L KH_2PO_4, 1.2 mmol/L $CaCl_2$, 20 mmol/L glucose, and 10 mmol/L HEPES, pH=7.3, and allowed to adhere at wells coated with 10 μg/mL Laminin (Sigma) for 1 hour at 4°C. Afterward, 8 cells per condition were incubated for 2 hours in normoglycemic (10 mmol/L) or hyperglycemic (50 mmol/L) medium in the presence or absence of HDL (5 μg/mL) (MP Biomedicals, Solon, Ohio) with the phosphatidylinositol-3 kinase (PI3K) inhibitor wortmannin (10 nmol/L) or the nitric oxide inhibitor N^G-nitro-L-arginine methyl ester (L-NAME; 100 nmol/L), and cardiomyocyte contractility was measured.

Ex Vivo Measurement of Cardiomyocyte Contractility

Single cardiomyocytes were field stimulated (1 Hz, 12 V). Resting cell length and cell shortening were measured with a videoimaging edge detector system (IonOptix, Milton, Mass).[18]

Plasma TBARS

The concentration of lipid peroxide was measured as TBARS as previously described.[4] Briefly, 25 μL plasma and the standard (diluted 1:3 in NaCl 0.9%) were incubated with 1.6 mL H_2SO_4 (0.042 mol/L) and 0.4 mL thiobarbituric acid (0.041 mol/L) in 50% acetic acid (Sigma) for 60 minutes at 90°C. After cooling in ice water, 2 mL n-butanol was added, and the mixture was shaken and centrifuged at 3000 U/min for 10 minutes. The butanol phase was used for measurement of TBARS fluorescence (excitation, 515 nm; emission, 533 nm). TBARS concentration was calculated with 1,1,3,3-tetraethoxypropane dissolved in acetic acid used as standard (Sigma).

Real-Time Reverse-Transcriptase Polymerase Chain Reaction Quantification of Antioxidative, Proinflammatory, Antiapoptotic, and Proapoptotic Genes

Quantitative real-time reverse-transcriptase polymerase chain reaction (ABI PRISM 7900 HT Sequence Detection System software version 2.2.2, PerkinElmer, Waltham, Mass) of 100 ng cDNA was used to quantify rat LV superoxide dismutase (SOD) *SOD-1*, *SOD-2*, *ec-SOD*, intracellular adhesion molecule-1 (*ICAM-I*), vascular cell adhesion molecule-1 (*VCAM-I*), tumor necrosis factor-α (*TNF-*α), *Bcl-2*, *Bax*, and *L32* cDNA levels (n=6 per group). The cDNA expression levels of these genes were normalized to *L32* cDNA. Conventional polymerase chain reaction products of rat *SOD-1*, *SOD-2*, *ec-SOD*, *ICAM-I*, *VCAM-I*, *TNF-*α, *Bcl-2*, *Bax*, and *L32* were obtained with the primers designed for real-time polymerase chain reaction and were cloned into pGEM-T Easy vector (Promega, Madison, Wis) to be used as DNA standards. The sequences of the primer sets used in this study were as follows: for SOD-1, 5′-CGGATGAAGAGAGGCATGTTG-3′ and 5′-TTGGCCACACC-GTCC TTT-3′; for SOD-2, 5′-GCCTCCCTGACCTGCCTTAC-3′ and 5′-GCATGAT CTGCGCTTAATG-3′; for ec-SOD, 5′-GG-AGATCTGG ATGGAGCTAGGA-3′ and 5′-CCTGCAGACTG-CGTGCAT-3′; for ICAM-1, 5′-GTCTCATGCCCGTGAAATT ATG-3′ and 5′-CATTTTCTCCCAGGCATTCTCT-3′; for VCAM-1, 5′-GGAGG TCTACTCATTCCCTGAAGA-3′ and 5′-ACCGTGCAGTTGACA GTGACA-3′; for TNF-α, 5′-AGACC-CTCACACTCAGATCATCTTC-3′ and 5′-CTCCGCTTGGT GGTTTGC-3′; for Bcl-2, 5′-GTTGCAGTCACCGGATTCCT-3′ and 5′-CGGA GGTGGTGTGAATCCA-3′; for Bax, 5′-GGGT-GGCAGCTGACATGTTT-3′ and 5′-GCCTTGAGCACCAGTTT-GC-3′; and for L32, 5′-AACCGAAAAGCCATCGTAGA AA-3′ and (reverse) 5′-CCTGGC GTTGGGATTGG-3′.

Azan Mallory Staining

Azan Mallory–stained sections were examined with a Leitz G20 microscope and examined at a calibrated magnification of ×400 with an ocular reticle containing 42 sampling points (Wild Heerburg Instruments, Geneva, Switzerland).[19] Thirty fields were evaluated in the endomyocardial, midmyocardial, and epimyocardial regions of each LV. To analyze the percentage of myocardial fibrosis, the number of points overlying the areas of collagen accumulation was quantified.

Periodic Acid–Schiff Staining

Periodic acid–Schiff–stained sections were quantified by digital image analysis.[20] The septum, right ventricle, and LV were measured. Perivascular glycogen accumulation was not analyzed. Glycogen accumulation is represented as percent of total area.

Western Blot

LV samples were homogenized in lysis buffer containing proteinase and phosphatase inhibitors. An equal amount of protein (10 to 30 μg) was loaded into a 10% SDS-PAGE. p38, phosphorylated (p) p38, Akt, p-Akt–Ser 473, glycogen synthase kinase (GSK), p-GSK–Ser 9, endothelial nitric oxide synthase (eNOS; Cell Signaling Technology, Danvers, Mass), p-eNOS–Ser 1177, and β tubulin (Santa Cruz Biotechnology, Santa Cruz, Calif) were detected with each specific antibody. The blots were visualized with a chemiluminescence system (Amersham Bioscience, Buckinghamshire, UK). Quantitative analysis of the intensity the bands was performed with NIH Image 1.63 software.

Caspase 3/7 Assay

LV caspase 3/7 activity was measured with a caspase-Glo 3/7 assay kit (Promega) according to the manufacturer's protocol. In brief, 100 μL vehicle or LV protein extracts (30 μg) were added to a white-walled 96-well luminometer plate. Then, 100 μL caspase-Glo 3/7 reagent containing caspase 3/7 buffer and the proluminescent caspase 3/7 substrate was added to each sample. After 1 hour of incubation at room temperature, the luminescence of each sample was measured in a microplate-reading luminometer (Berthold Detection Systems, Oak Ridge, Tenn).

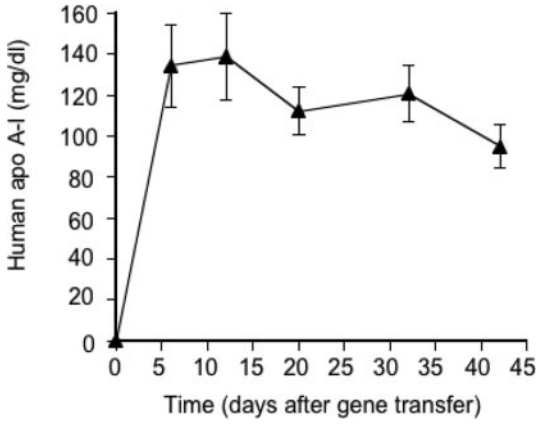

Figure 1. Time course of human apoA-I expression after *Ad.hapoA-I* GT in streptozotocin-induced diabetic rats. Data represent mean±SEM of 5 different rats.

Immunofluorescence Staining

Serial 4-μm-thick transverse sections were embedded in paraffin for subsequent immunohistochemical analyses. The primary antibodies used were as follows: rabbit monoclonal anti–phospho-Akt-Ser 473 (dilution, 1:25; Cell Signaling Technology) and mouse monoclonal anti–α-sarcomeric actin (dilution, 1:30; Sigma) to recognize cardiomyocytes and mouse monoclonal anti-platelet/endothelial cell adhesion molecule 1/CD31 (dilution, 1:50; AbD Serotec, Dusseldorf, Germany) to detect endothelial cells. FITC-labeled IgG and tetramethylrhodamin isothiocyanate–labeled IgG were used as secondary antibodies (dilution, 1:200; Sigma). Nuclei were stained with 4′,6-diamino-2-phenylindole (DAPI; dilution, 1:200). Finally, sections were mounted and examined under a fluorescence microscope (Leica). To exclude any cardiac tissue cross-reactivity, isotype-matched negative controls were used and showed no positive staining.

Annexin V Staining of Rat Cardiomyocytes

Freshly isolated cardiomyocytes from adult male SD rats were allowed to adhere for 1 hour at 4°C on coverslips in 6-well plates. Adherent cells were incubated for 2 hours in modified Krebs-Henseleit buffer (normoglycemic, 10 mmol/L glucose) or in the presence of 50 mmol/L glucose (hyperglycemic) with or without HDL (1 μg/mL) (MP Biomedicals), wortmannin (100 nmol/L), or L-NAME (100 nmol/L). For detection, coverslips were mounted for 10 minutes with 100 μL annexin V solution (Roche, Mannheim, Germany) including 1 μg/mL propidium iodide (Sigma). Coverslips were placed on slides and examined under a Leica DMLB (Zeiss, Jena, Germany) fluorescence microscope at 488 nm. Incubation was carried out in duplicate, and apoptotic (green fluorescence), necrotic (green fluorescence with red fluorescent nucleus), and living (no fluorescence) cells were counted for at least 6 visual fields. Pictures were taken and analyzed with the software AxioVision 4.3 (Carl Zeiss Vision GmbH, Aalen, Germany). Data are given as mean±SEM of counted cells in 4 slides and depicted as x-fold of the normoglycemic control group set as 1.

Electron Microscopy

After fixation in Karnovsky fixative followed by postfixation in 1% osmium tetroxide solution (0.1 mol/L phosphate buffer), small pieces of LV were rinsed and dehydrated in ascending alcohol series as described by Shakibaei.[21] Next, samples were embedded in Epon and cut on a Reichert-Jung Ultracut E (Nussloch, Germany), followed by contrasting with 2% uranyl acetate/lead citrate. A transmission electron microscope (Zeiss TEM 10) was used to examine

Table 1. Metabolic Parameters

	SD-*Ad.Null*	STZ-*Ad.Null*	STZ-*Ad.hapoA-I*
Blood glucose, mg/dL	183±12	957±41*	1031±32*
Total cholesterol, mg/dL	35±2.8	140±8.1*	130±7.6*
VLDL-C, mg/dL	3.1±0.53	27±1.9*	15±1.7*†
IDL-C, mg/dL	1.1±0.071	30±4.4*	16±1.7*‡
LDL-C, mg/dL	2.7±0.3	40±4.4*	31±4.1*
HDL-C, mg/dL	28±2.5	42±2.4*	68±5.1*†
Non–HDL-C/HDL-C	0.26±0.021	2.4±0.28*	0.97±0.11*†
Triglycerides, mg/dL	77±11	990±170*	360±65*‡

Data are given as mean±SEM. n=8 per group.
*$P<0.005$ vs SD-*Ad.Null*; †$P\leq0.0005$ vs STZ-*Ad.Null*; ‡$P<0.01$ vs STZ-*Ad.Null*.

the sections. To assess the number of cardiomyocytes with morphological features of apoptotic cell death and the number of changed endothelial cells with changed basement membrane, which was determined by scoring 100 cells from 20 different microscopic fields, ultrathin sections of the samples were prepared and evaluated with an electron microscope (Zeiss EM 10).

Statistical Analysis

Data are presented as mean±SEM. Paired and unpaired Student's *t* tests or 1-way ANOVA for comparisons among multiple groups was used for statistical analysis. Differences were considered significant at $P<0.05$.

The authors had full access to and take full responsibility for the integrity of the data. All authors have read and agree to the manuscript as written.

Results

Increase of HDL via Human ApoA-I GT

To investigate whether increased HDL-C may affect the development of diabetic cardiomyopathy, GT was performed with a human apoA-I–expressing adenoviral vector (*Ad.hapoA-I*)[15] 5 days after diabetes induction via intraperitoneal streptozotocin injection. GT resulted in sustained expression of human apoA-I for the entire duration of the experiment, 6 weeks, with expression levels >95 mg/dL (Figure 1), and did not lead to a significant alteration of alanine aminotransferase or aspartate aminotransferase levels at any time point after GT (data not shown). HDL-C levels were increased 1.6-fold ($P<0.001$) at the day of death (day 42) compared with diabetic controls injected with the *Ad.Null* vector[15] containing no expression cassette (Table 1). VLDL-C and IDL-C were significantly lower in *Ad.hapoA-I*–treated rats than in *Ad.Null*–injected rats, whereas LDL-C was not significantly changed (Table 1). The reduction in VLDL-C and IDL-C after *Ad.hapoA-I* GT was paralleled by a 2.8-fold reduction in triglycerides ($P<0.005$). On the other hand, increased HDL-C levels did not affect blood glucose levels (Table 1).

ApoA-I GT Improves Cardiomyocyte Contractility

The contractility parameters dP/dtmax and dP/dtmin were significantly impaired (31.1% and 47.5%, respectively;

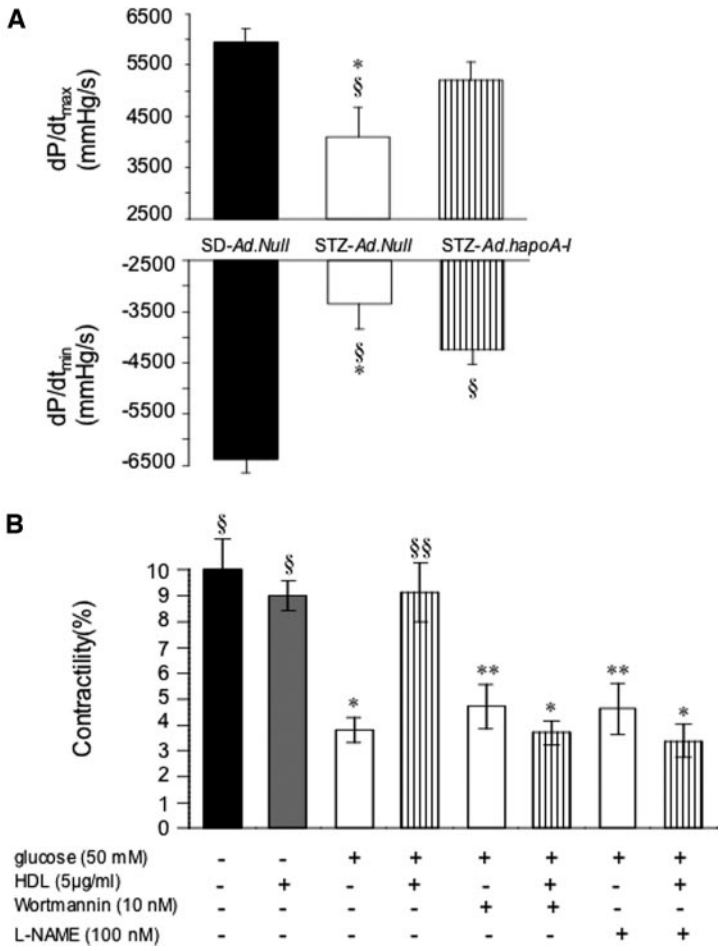

Figure 2. ApoA-I GT improves contractility parameters in streptozotocin-induced diabetic cardiomyopathy. A, Bar graphs representing contractility parameters dP/dtmax and dP/dtmin. Data are depicted as mean±SEM. *$P<0.05$ vs STZ-*Ad.hapoA-I*, §$P<0.005$ vs SD-*Ad.Null* (SD-*Ad.Null*, n=12; STZ-*Ad.Null*, n=7; STZ-*Ad.hapoA-I*, n=13). B, Bar graphs representing contractility (%) of cardiomyocytes isolated from SD rats and ex vivo incubated for 2 hours in indicated media. Data are depicted as mean±SEM. *$P<0.0005$, **$P<0.005$ vs normal; §$P<0.0005$, §§$P<0.001$ vs hyperglycemia (n=8 cells).

Table 2. Heart Morphology

	SD-*Ad.Null*	STZ-*Ad.Null*	STZ-*Ad.hapoA-I*
BW, g	489±12	246±6.8*	250±5.2*
HW, mg	1205±29.5	847±17.7*	831±19.3*
LVW, mg	874±19.0	580±16.9*	595±16.7*
HW/BW $\times 10^{-3}$	2.48±0.05	3.46±0.09*	3.32±0.07*
LVW/HW	0.724±0.01	0.683±0.01†	0.716±0.01

BW indicate body weight; HW, heart weight; and LVW, LV weight. Data are given as mean±SEM. SD-*Ad.Null*, n=17; STZ-*Ad.Null*, n=13; STZ-*Ad.hapoA-I*, n=16.

*$P<0.005$ vs SD-*Ad.Null*; †$P<0.05$ vs SD-*Ad.Null* and STZ-*Ad.hapoA-I*.

$P<0.005$) in streptozotocin-*Ad.Null* (STZ-*Ad.Null*) rats compared with nondiabetic controls. In contrast, human apoA-I GT resulted in a 27.2% ($P<0.05$) increase in dP/dtmax and a 26.8% ($P<0.05$) decrease in dP/dtmin compared with the STZ-*Ad.Null* group (Figure 2A). Human apoA-I GT did not affect body weight, heart weight, and LV weight of streptozotocin rats (Table 2).

To investigate whether human apoA-I GT in streptozotocin-induced diabetic rats leads to an improvement in cardiomyocyte contractility via a direct positive effect of HDL on cardiomyocytes, an ex vivo experiment was conducted with adult cardiomyocytes isolated from SD rats incubated in normoglycemic or hyperglycemic medium in the presence or absence of HDL. Supplementation of HDL in normoglycemic medium did not affect cardiomyocyte contractility, whereas under hyperglycemic conditions, HDL could overcome the glucose-induced reduction in contractility. This HDL-mediated effect was abolished in the presence of wortmannin or L-NAME (Figure 2B).

ApoA-I GT Reduces Oxidative Stress

The severe hyperglycemic state of streptozotocin-induced diabetes is associated with the formation of reactive oxygen species such as superoxide (O_2^-)[22] and TBARS.[4] We investigated whether apoA-I GT via the antioxidative properties of HDL[9,23] could reduce oxidative stress, systemically and locally, in the heart. We found that apoA-I GT in streptozotocin rats resulted in a 2.4-fold ($P<0.05$) decrease in serum TBARS levels (Figure 3A). In the heart, apoA-I GT led to a decrease in oxidative stress, as evidenced by a 1.5-fold ($P<0.05$) reduced activated phosphorylation state of the stress-induced p38 mitogen-activated protein kinase (MAPK) compared with STZ-*Ad.Null* controls (Figure 3B) and an induction of the antioxidant enzyme SOD. Specifically, apoA-I GT increased diabetes-downregulated *SOD-2* 1.2-fold ($P<0.05$) and normalized *ec-SOD* expression to levels found in nondiabetic controls without affecting *SOD-1* expression (Figure 3C).

ApoA-I GT Reduces Cardiac Inflammation

Given the well-known antiinflammatory properties of HDL,[11,24] we further analyzed the effect of human apoA-I GT on cardiac inflammation. ApoA-I GT resulted in a significant decrease in diabetes-induced LV *ICAM-1*, *VCAM-1*, and *TNF-α* mRNA expression to levels not significantly different from nondiabetic *Ad.Null* controls (Figure 3D).

ApoA-I GT Reduces Cardiac Fibrosis and Glycogen Accumulation

Because cardiac hemodynamics are affected by changes in collagen content, total collagen content was analyzed in the hearts. Total collagen content increased by 2.0-fold ($P<0.05$) in STZ-*Ad.Null* hearts compared with nondiabetic *Ad.Null* controls, whereas apoA-I GT in streptozotocin rats reduced cardiac fibrosis by 1.7-fold ($P<0.05$) compared with STZ-*Ad.Null* rats (Figure 4A and 4C). The ratio of p-GSK to GSK was 2.4-fold ($P<0.0005$) higher in STZ-*Ad.hapoA-I* rat hearts than in STZ-*Ad.Null* rat hearts (Figure 4E). In agreement, glycogen accumulation in STZ-*Ad.hapoA-I* rat hearts was 3.1-fold ($P<0.05$) less abundant than in STZ-*Ad.Null* rat hearts (Figure 4B and 4D).

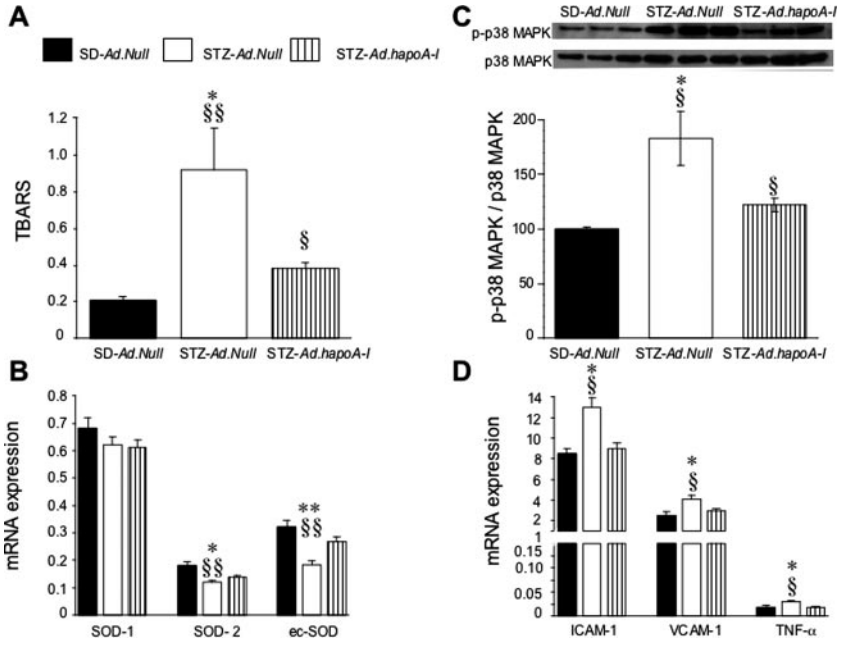

Figure 3. ApoA-I GT reduces oxidative stress and inflammation in streptozotocin-induced diabetic cardiomyopathy. A, Bar graph representing serum TBARS. B, Representative Western blots of phosphorylated p38 MAPK and p38 MAPK in the LV. Bar graph of the ratio of phosphorylated p38 MAPK to p38 MAPK obtained by densitometric scanning of Western blots and expressed as the percentage of the nondiabetic control group SD-*Ad.Null* (n=4 for each condition). C, Bar graph representing LV *SOD-1*, *SOD-2*, and *ec-SOD* mRNA expression normalized to ribosomal *L32*. D, Bar graph representing LV *ICAM-1*, *VCAM-1*, and *TNF-α* mRNA expression normalized to ribosomal L32. Data are depicted as mean±SEM. §$P<0.05$, §§$P<0.005$ vs SD-*Ad.Null*; *$P<0.05$, **$P<0.005$ vs STZ-*Ad.hapoA-I*.

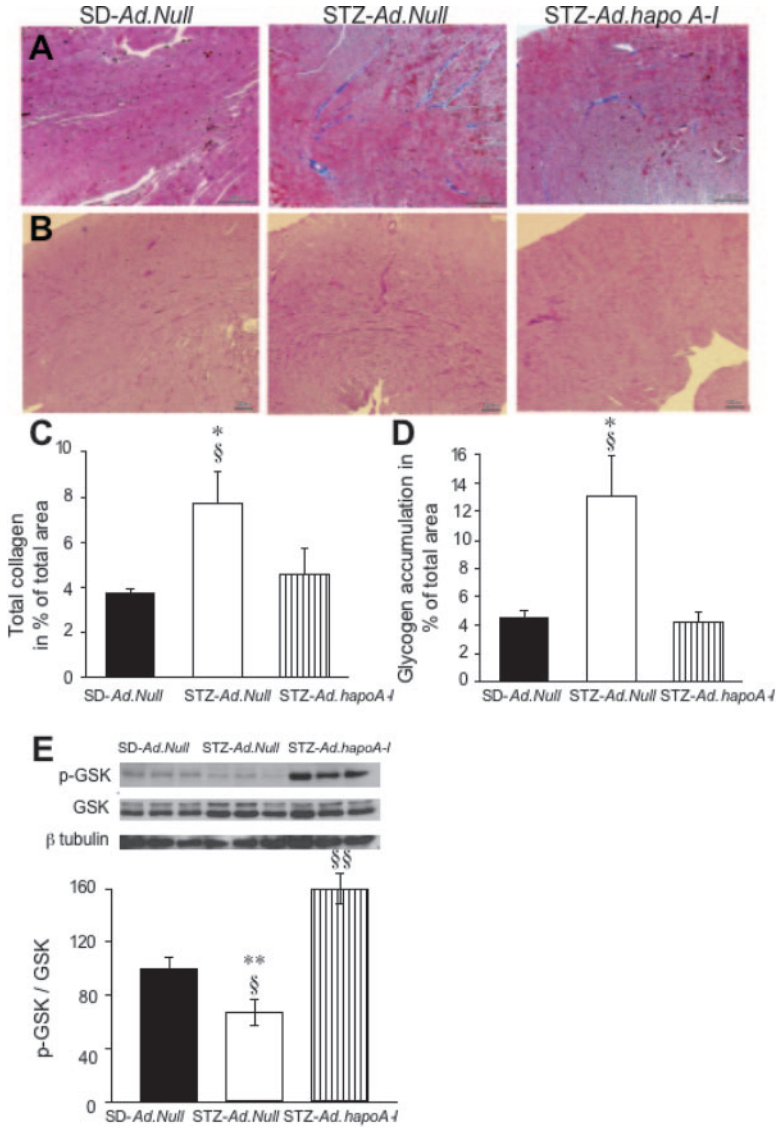

Figure 4. ApoA-I GT reduces cardiac fibrosis and glycogen accumulation in streptozotocin-induced diabetic cardiomyopathy. Representative pictures of Azan Mallory (A) and periodic acid–Schiff (B) stainings of SD-*Ad.Null*, STZ-*Ad.Null*, and STZ-*Ad.hapo A-I* hearts as indicated. Magnification ×50. Bar graphs represent collagen content (C) and glycogen accumulation (D) in percent total area. E, Representative Western blots of p-GSK, GSK, and β tubulin in the LV. Bar graph of the ratio of p-GSK to GSK obtained by densitometric scanning of Western blots and expressed as the percentage of the nondiabetic control group SD-*Ad.Null* (n=4 for each condition). Data are represented as mean±SEM. §$P<0.05$, §§$P<0.005$ vs SD-*Ad.Null*; *$P<0.05$, **$P<0.0005$ vs STZ-*Ad.hapoA-I*.

ApoA-I GT Reduces Cardiac Apoptosis and Protects Endothelial Integrity

Both inflammation and oxidative stress are known to contribute to apoptosis.[25] We hypothesized that reduced cardiac inflammation and oxidative stress after human apoA-I GT may decrease cardiac apoptosis. Therefore, we first investigated the effect of human apoA-I GT on the activity of the downstream caspase 3 and 7. We found that caspase 3/7 activity was 1.2-fold ($P<0.05$) reduced after apoA-I GT compared with diabetic controls (Figure 5A). To further assess the impact of apoA-I GT on cardiomyocyte survival, we analyzed the expression of the antiapoptotic Bcl-2 and the proapoptotic Bax, the ratio of which represents an important marker of cardiomyocyte survival probability.[26] In addition, we analyzed the phosphorylation state of the protein kinase B Akt, a critical regulator of cell survival,[27] and of its downstream effector, eNOS, and examined the localization of phosphorylated Akt in the heart. ApoA-I GT increased *Bcl-2* mRNA expression by 1.6-fold ($P<0.005$) (SD-*Ad.Null*, 0.021±0.0032; STZ-*Ad.Null*, 0.013±0.0013; STZ-*Ad.hapoA-I*, 0.020±0.0016), whereas the expression of the proapoptotic *Bax* was not different between the different groups. As a result, apoA-I GT increased the ratio of *Bcl-2* to *Bax* by 1.9-fold ($P<0.005$) compared with STZ-*Ad.Null* rats (Figure 5B). p-Akt (nuclear/cytoplasmatic[28]) was found to be present in cardiomyocytes and in cardiac endothelial cells (Figure 6). ApoA-I GT increased the diabetes-downregulated ratio of p-Akt to Akt by 1.6-fold ($P<0.0005$), leading to a ratio not significantly different from nondiabetic controls (Figure 5C). This was paralleled by a 1.6-fold ($P<0.005$) increase in the ratio of p-eNOS to eNOS (Figure 5D). Moreover, apoA-I GT normalized the diabetes-downregulated expression of eNOS (SD-*Ad.Null*, 100±7; STZ-*Ad.Null*, 72±2.5; STZ-*Ad.hapoA-I*, 96±4.4, expressed as percent versus SD-*Ad.Null*).

To further investigate the antiapoptotic potential of HDL and its underlying pathways on cardiomyocytes in the diabetic heart, HDL was supplemented for 2 hours to freshly isolated rat cardiomyocytes under hyperglycemic conditions in the presence or absence of wortmannin or L-NAME. HDL decreased the amount of hyperglycemia-induced apoptotic cardiomyocytes by 3.4-fold ($P<0.005$) compared with glucose, whereas it did not affect the amount of necrotic cells. The antiapoptotic effect of HDL was blunted in the presence

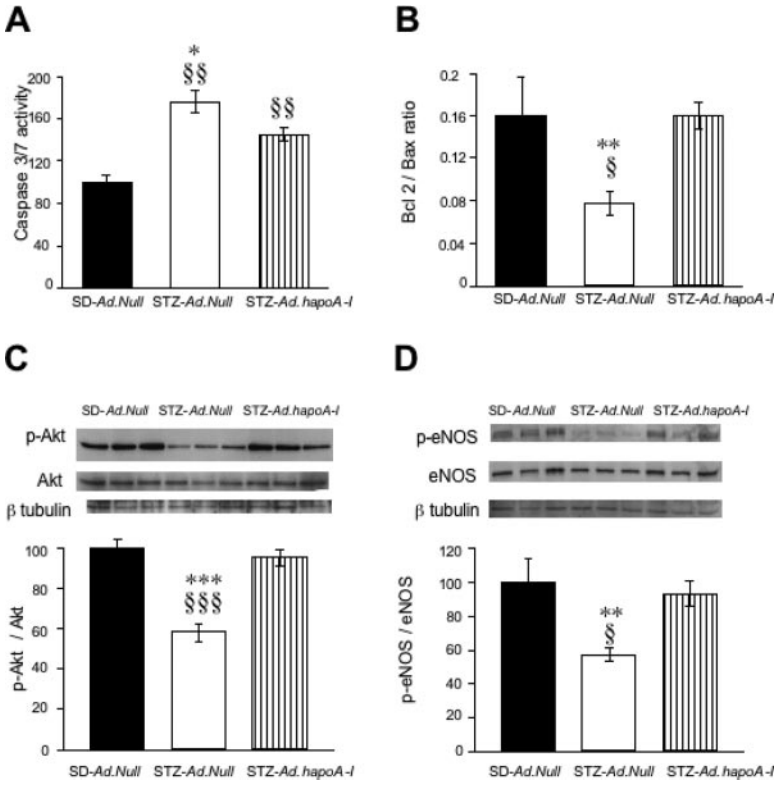

Figure 5. ApoA-I GT reduces apoptosis in streptozotocin-induced diabetic cardiomyopathy. A, Bar graphs representing LV caspase 3/7 activity as the percentage of the nondiabetic control group SD-*Ad.Null*. B, Ratio of Bcl-2 to Bax of SD-*Ad.Null*, STZ-*Ad.Null*, and STZ-*Ad.hapoA-I*. Representative Western Blots of p-Akt, Akt, and β tubulin (C) and p-eNOS, eNOS, and β tubulin (D) in the LV. Bar graphs of the ratios of p-Akt to Akt (C) and p-eNOS to eNOS (D) obtained by densitometric scanning of Western blots and expressed as the percentage of the nondiabetic control group SD-*Ad.Null* (n=4 for each condition). Data are represented as mean±SEM. §$P<0.05$, §§$P<0.005$, §§§$P<0.0005$ vs SD-*Ad.Null*; *$P<0.05$, **$P<0.005$, ***$P\leq0.0005$ vs STZ-*Ad.hapoA-I*.

of wortmannin or L-NAME (Figure 7). To further evaluate the effects of apoA-I GT on the cellular ultrastructure of the cardiomyocytes and cardiac endothelium in the diabetic myocardium, samples from the LV of nondiabetic SD-*Ad.Null*, diabetic STZ-*Ad.Null* controls, and diabetic rats that underwent apoA-I GT were examined by electron microscopy (Figure 8A through 8F). Compared with nondiabetic controls, STZ-*Ad.Null* rats revealed a significantly higher number of cells with mitochondrial changes and apoptotic bodies, whereas the total number of cardiomyocytes with apoptotic characteristics was 2.1-fold ($P<0.05$) reduced in STZ-*Ad.hapoA-I* rats (Figure 8G). In parallel, the number of disrupted endothelial cells with changed (disrupted/swollen) basement membrane was 21-fold ($P<0.0005$) increased in STZ-*Ad.Null* versus SD-*Ad.Null* rats, whereas apoA-I GT resulted in 3.0-fold ($P<0.005$) -lower damaged endothelial cells and basement membrane compared with STZ-*Ad.Null* rats (Figure 8H).

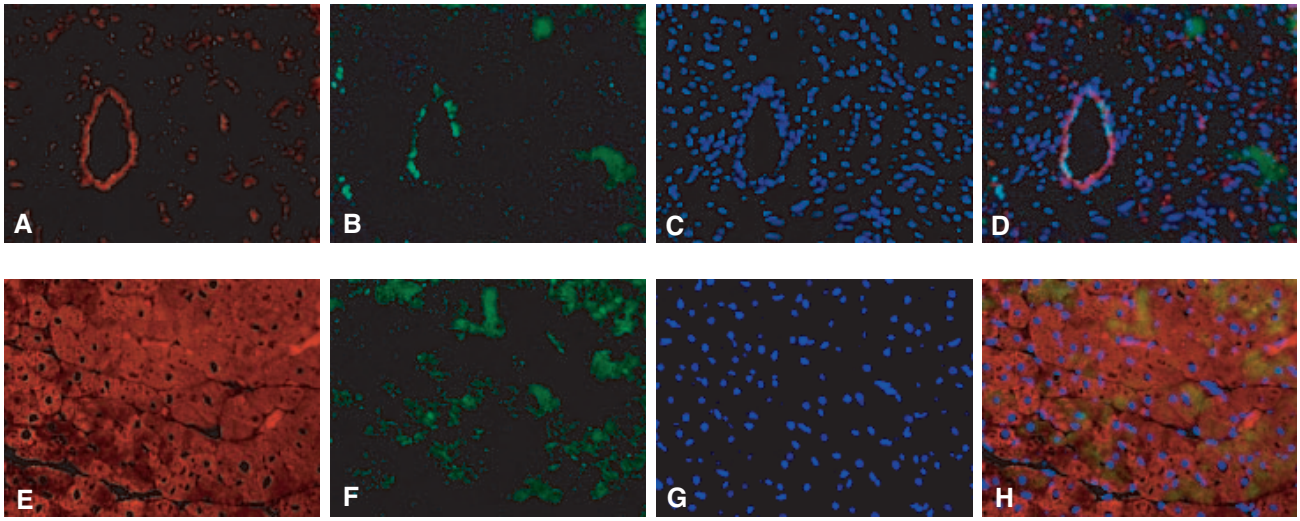

Figure 6. Cardiac cellular sources of phospho-Akt. The representative immunofluorescence stainings on the same section from a SD-*Ad.Null* rat showed that specific signals for nuclear (DAPI, blue; C and G) and cytoplasmatic p-Akt (green; B and F) were detected in both CD31+ (red; A) endothelial cells (A through D; magnification ×400) and α-sarcomeric actin+ (red; E) cardiomyocytes (E through H; magnification ×500), respectively. D, H, Merged pictures of CD31, p-Akt, and DAPI (D) and α-sarcomeric actin+, p-Akt, and DAPI stainings (H).

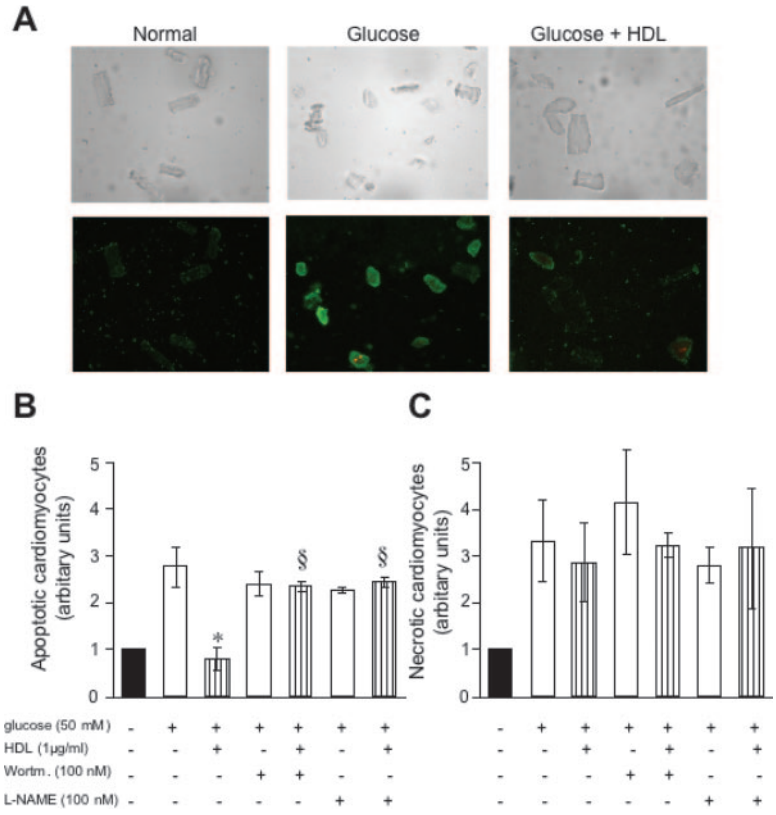

Figure 7. HDL reduces hyperglycemia-induced cardiomyocyte apoptosis ex vivo. A, Representative phase contrast (top) and fluorescent (bottom) pictures of cardiomyocytes isolated from SD rats and ex vivo incubated for 2 hours in normoglycemic medium (normal), hyperglycemic medium (glucose), and hyperglycemic medium in the presence of HDL (glucose+HDL) as indicated. Magnification ×200. Bar graphs representing annexin V–positive cells, defined as apoptotic cells (B), and annexin V–positive and propidium iodide–positive cells, defined as necrotic cells (C), of cardiomyocytes isolated from SD rats and ex vivo incubated for 2 hours in indicated media. Data are represented as mean±SEM of counted cells in 4 slides and depicted as x-fold of the normoglycemic control group set as 1. *P=0.005 vs glucose; §P<0.005 vs glucose+HDL.

Discussion

Our study reveals that apoA-I GT reduces the development of experimental diabetic cardiomyopathy via reduction of cardiac oxidative stress, inflammation, fibrosis, apoptosis, and glycogen accumulation despite severe hyperglycemia and unaltered levels of LDL-C.

Effect of ApoA-I GT on Oxidative Stress, Inflammation, and Fibrosis

Hyperglycemia induces oxidative stress by inducing the generation of reactive oxygen species on the one hand and reducing the production of antioxidant enzymes on the other hand.[29] In this study, we demonstrate that apoA-I GT resulted in a systemic reduction in oxidative stress by decreasing TBARS levels. Besides inducing lipid peroxidation, reactive oxygen species can alter cellular proteins and initiate diverse stress-signaling pathways like Erk, jun N-terminal kinase, and p38 MAPK. We recently demonstrated that p38 MAPK inhibition improves LV dysfunction in streptozotocin-induced diabetic mice,[30] indicating the pathological importance of p38 MAPK in the diabetic heart. Therefore, we focused on analyzing the effect of apoA-I GT in streptozotocin rats on the activated phosphorylation state of the stress-activated MAPK p38 and found a significant reduction. Because p38 MAPK also is known to activate nuclear factor-κB, which in turn regulates the expression of proinflammatory cytokines, cell adhesion molecules, and others, the reduced activation of p38 MAPK may have contributed to the decreased inflammation observed after apoA-I GT. On the other hand, the antiinflammatory properties of HDL[11,24] may have directly contributed to the decreased cell adhesion molecules and TNF-α expression. We further analyzed the effect of apoA-I GT on the cardiac expression of the 3 forms of the antioxidant enzyme SOD, SOD-1, SOD-2, and ec-SOD, which convert O_2^- anions into molecular oxygen and hydrogen peroxide. Their importance for the heart has been outlined in transgenic and knockout animal models[31] and recently for SOD-2 in a diabetic setting.[32] In the streptozotocin-induced diabetic heart, we found a downregulation of *SOD-2* and *ec-SOD* mRNA expression, whereas *SOD-1* mRNA expression was unaltered compared with nondiabetic controls. ApoA-I GT resulted in an increase in diabetes-downregulated SOD-2 expression and normalized diabetes-reduced ec-SOD expression to levels found in nondiabetic controls. The latter finding and the unchanged SOD-1 expression are in line with the findings of Kruger et al,[22] who found an increase in ec-SOD in the aorta of streptozotocin-induced diabetic rats after administration of the apoA-I mimetic peptide D-4F and no regulation of SOD-1. In the heart, overexpression of ec-SOD has been shown to decrease macrophage infiltration and fibrosis and to improve LV dysfunction,[31] whereas overexpression of SOD-2 has been shown to protect mitochondrial respiratory function and to block apoptosis induction.[33] These studies suggest that the reduced cardiac fibrosis after apoA-I GT in streptozotocin rats can be explained by the decreased oxidative stress and inflammation, including downregulated expression of profibrotic cytokines like TNF-α[4] (inflammatory fibrosis), as well as by a reduction in cardiac apoptosis (see above) and subsequent replacement fibrosis, leading to improved LV function.

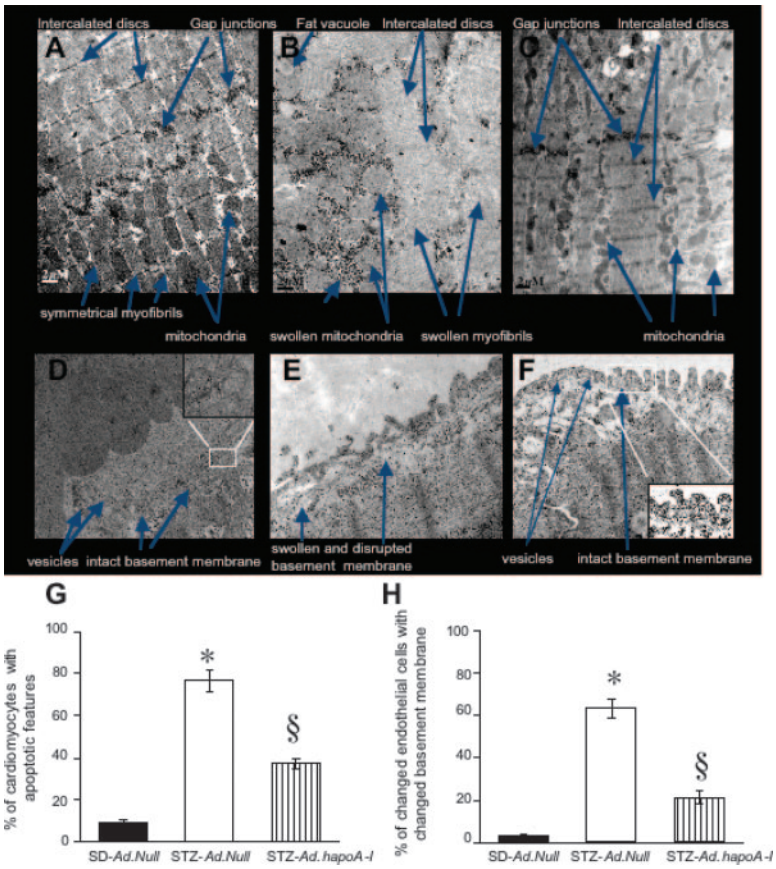

Figure 8. Ultrastructural morphology of cardiomyocytes and cardiac endothelium. Representative transmission electron micrographs of LV specimens from SD-*Ad.Null* (A and D), STZ-*Ad.Null* (B and E), and STZ-*Ad.hapoA-I* (C and F) rats. Well-organized, typical symmetric myofibrils with packed mitochondria beside the fibers are found in SD-*Ad.Null* rats (A), whereas disorganized swollen fibrils and swollen mitochondria are evident in STZ-*Ad.Null* rats (B). Less swollen actin-myosin filaments and mitochondria are present in STZ-*Ad.hapoA-I* rats vs STZ-*Ad.Null* (C). The extensive accumulation of glycogen evident in STZ-*Ad.Null* rats (B) is reduced in STZ-*Ad.hapoA-I* rats (C). Intact endothelial cells and basement membranes are found in SD-*Ad.Null* rats (D), whereas disrupted endothelial cells and basement membranes are present in STZ-*Ad.Null* rats (E). Less disrupted membranes are present in STZ-*Ad.hapoA-I* rats vs STZ-*Ad.Null* (F). G and H, The frequency of the number of cardiomyocytes with mitochondrial changes, apoptotic bodies, and the number of endothelial cells with changes in basement membrane in SD-*Ad.Null*, STZ-*Ad.Null*, and STZ-*Ad.hapoA-I* rats was evaluated by scoring 100 cells from 20 different microscopic fields in each condition. Bar graphs highlight the percent of cardiomyocytes with altered mitochondria and nuclei (G) and the percent of changed endothelial cells with changed basement membrane (H). Data are represented mean±SEM (n=3 independent experiments). Magnification ×5000; inset magnification ×20 000. *$P<0.05$ vs SD-*Ad.Null* and STZ-*Ad.hapoA-I*; §$P<0.05$ vs SD-*Ad.Null* and STZ-*Ad.Null*.

Effect of ApoA-I GT on Cardiac Apoptosis and Glycogen Accumulation

The incidence of apoptosis increases in the heart of diabetic patients[34] and streptozotocin-induced diabetic animals[6] and is directly linked to hyperglycemia-induced oxidative stress.[6] Mitochondria play an important role in oxidative stress–induced apoptosis, and caspase 3 and 7 are essential mediators in the mitochondrial processes of apoptosis.[35] In streptozotocin-induced diabetic rats, we found an upregulation of caspase 3/7 activity, which was reduced after apoA-I GT. In addition, apoA-I GT normalized the diabetes-reduced mRNA expression of the antiapoptotic *Bcl-2*, a "guardian" against mitochondrial initiation of caspase activation,[36] to levels found in nondiabetic hearts and tended to reduce the expression of the proapoptotic Bax. This resulted in an increased ratio of Bcl-2 to Bax, which has been reported to be a marker of increased cardiomyocyte survival probability.[26] Moreover, apoA-I GT normalized the diabetes-reduced phosphorylation/activation state of the protein kinase B Akt[13] and of its effector eNOS to levels found in nondiabetic hearts. However, this was not associated with a complete rescue of our animal model, indicating the multifactorial pathogenesis of the disorder. Immunofluorescence staining illustrated the presence of activated Akt in cardiomyocytes and cardiac endothelial cells. Because Akt is a critical regulator of cell survival,[27] these findings may contribute to the reduction in cardiomyocyte apoptosis and the improvement in endothelial integrity found in the STZ-*Ad.hapoA-I* rat hearts (see above). The antiapoptotic effect of HDL on cardiomyocytes under hyperglycemia has been confirmed ex vivo, showing that HDL supplementation on cardiomyocytes in hyperglycemia reduces apoptosis. In agreement with the increased phosphorylation state of Akt and eNOS in STZ-*Ad.hapoA-I* rat hearts, supporting a HDL-Akt-eNOS pathway, the antiapoptotic effect of HDL was found to be PI3K and nitric oxide dependent. In addition, apoA-I GT also increased the diabetes-reduced phosphorylation/inactivation state of GSK-3β,[13,37] which was associated with less glycogen accumulation in the myocardium. On the ultrastructural level, these antiapoptotic effects of apoA-I GT were translated into a reduced number of cardiomyocytes with swollen mitochondria and apoptotic bodies. In addition, apoA-I GT led to an improved connected structure of the sarcomere (actin-myosin filaments), sharper intercalated disks, more intact endothelium and basement membrane, and less cardiac fibrosis and glycogen accumulation. We suggest that the combination of these effects on the different compartments of the heart (cardiomyocytes, cardiac endothelium, and extracellular matrix) contribute to the improved cardiac function found after apoA-I GT compared with streptozotocin-induced diabetic rats. In addition, although HDL had no effect on the contractility of isolated cardiomyocytes under control conditions, HDL improved their function under hyperglycemia-induced stress. This effect was PI3K and nitric oxide dependent. In summary, besides beneficial vasculoprotective/cardioprotective long-term effects, including an improvement in cardiac, vascular, and matrix remodeling, direct myocardial effects of HDL also may contribute to the improvement in cardiac function under severe streptozotocin-induced stress.

Conclusions

ApoA-I GT reduces the development of experimental diabetic cardiomyopathy, leading to improved LV function. This study, performed in an animal model characterized by severe hyperglycemia, oxidative stress, and a ratio of HDL-C to LDL-C of 1, strongly suggests that HDL has direct cardioprotective effects. However, the relevance of the use of HDL-raising therapies for the cotreatment of diabetic cardiomyopathy should be examined in future studies that also investigate the effect of increasing HDL on established diabetic cardiomyopathy.

Sources of Funding

This study was supported by grants from the European Foundation for the Study of Diabetes to Drs Tschöpe and Van Linthout, the Sonderforschungsbereich Transregio-19 Project Z3 to Dr Tschöpe, and the Sonderforschungsbereich Transregio-19 Project C2 to Dr Felix. The Center for Molecular and Vascular Biology (Drs Lievens and De Geest) is supported by the Excellentiefinanciering KU Leuven (EF/05/013).

Disclosures

None.

References

1. Poornima IG, Parikh P, Shannon RP. Diabetic cardiomyopathy: the search for a unifying hypothesis. *Circ Res*. 2006;98:596–605.
2. Kajstura J, Fiordaliso F, Andreoli AM, Li B, Chimenti S, Medow MS, Limana F, Nadal-Ginard B, Leri A, Anversa P. IGF-1 overexpression inhibits the development of diabetic cardiomyopathy and angiotensin II-mediated oxidative stress. *Diabetes*. 2001;50:1414–1424.
3. Tschope C, Walther T, Koniger J, Spillmann F, Westermann D, Escher F, Pauschinger M, Pesquero JB, Bader M, Schultheiss HP, Noutsias M. Prevention of cardiac fibrosis and left ventricular dysfunction in diabetic cardiomyopathy in rats by transgenic expression of the human tissue kallikrein gene. *FASEB J*. 2004;18:828–835.
4. Tschope C, Walther T, Escher F, Spillmann F, Du J, Altmann C, Schimke I, Bader M, Sanchez-Ferrer CF, Schultheiss HP, Noutsias M. Transgenic activation of the kallikrein-kinin system inhibits intramyocardial inflammation, endothelial dysfunction and oxidative stress in experimental diabetic cardiomyopathy. *FASEB J*. 2005;19:2057–2059.
5. Devereux RB, Roman MJ, Paranicas M, O'Grady MJ, Lee ET, Welty TK, Fabsitz RR, Robbins D, Rhoades ER, Howard BV. Impact of diabetes on cardiac structure and function: the Strong Heart Study. *Circulation*. 2000;101:2271–2276.
6. Cai L, Li W, Wang G, Guo L, Jiang Y, Kang YJ. Hyperglycemia-induced apoptosis in mouse myocardium: mitochondrial cytochrome C-mediated caspase-3 activation pathway. *Diabetes*. 2002;51:1938–1948.
7. Gordon T, Castelli WP, Hjortland MC, Kannel WB, Dawber TR. High density lipoprotein as a protective factor against coronary heart disease: the Framingham study. *Am J Med*. 1977;62:707–714.
8. Rubins HB, Robins SJ, Collins D, Fye CL, Anderson JW, Elam MB, Faas FH, Linares E, Schaefer EJ, Schectman G, Wilt TJ, Wittes J. Gemfibrozil for the secondary prevention of coronary heart disease in men with low levels of high-density lipoprotein cholesterol: Veterans Affairs High-Density Lipoprotein Cholesterol Intervention Trial Study Group. *N Engl J Med*. 1999;341:410–418.
9. Mackness MI, Durrington PN. HDL, its enzymes and its potential to influence lipid peroxidation. *Atherosclerosis*. 1995;115:243–253.
10. Sugano M, Tsuchida K, Makino N. High-density lipoproteins protect endothelial cells from tumor necrosis factor-alpha-induced apoptosis. *Biochem Biophys Res Commun*. 2000;272:872–876.
11. Cockerill GW, Huehns TY, Weerasinghe A, Stocker C, Lerch PG, Miller NE, Haskard DO. Elevation of plasma high-density lipoprotein concentration reduces interleukin-1–induced expression of E-selectin in an in vivo model of acute inflammation. *Circulation*. 2001;103:108–112.
12. Mineo C, Yuhanna IS, Quon MJ, Shaul PW. High density lipoprotein-induced endothelial nitric-oxide synthase activation is mediated by Akt and MAP kinases. *J Biol Chem*. 2003;278:9142–9149.
13. Montanari D, Yin H, Dobrzynski E, Agata J, Yoshida H, Chao J, Chao L. Kallikrein gene delivery improves serum glucose and lipid profiles and cardiac function in streptozotocin-induced diabetic rats. *Diabetes*. 2005;54:1573–1580.
14. Tschope C, Walther T, Yu M, Reinecke A, Koch M, Seligmann C, Heringer SB, Pesquero JB, Bader M, Schultheiss H, Unger T. Myocardial expression of rat bradykinin receptors and two tissue kallikrein genes in experimental diabetes. *Immunopharmacology*. 1999;44:35–42.
15. Van Linthout S, Lusky M, Collen D, De Geest B. Persistent hepatic expression of human apoA-I after transfer with a helper-virus independent adenoviral vector. *Gene Ther*. 2002;9:1520–1528.
16. De Geest B, Van Linthout S, Collen D. Sustained expression of human apoA-I following adenoviral gene transfer in mice. *Gene Ther*. 2001;8:121–127.
17. Chapman MJ, Goldstein S, Lagrange D, Laplaud PM. A density gradient ultracentrifugal procedure for the isolation of the major lipoprotein classes from human serum. *J Lipid Res*. 1981;22:339–358.
18. Bramlage P, Joss G, Staudt A, Jarrin A, Podlowski S, Baumann G, Stangl K, Felix SB, Stangl V. Computer-aided measurement of cell shortening and calcium transients in adult cardiac myocytes. *Biotechnol Prog*. 2001;17:929–934.
19. Anversa P, Palackal T, Sonnenblick EH, Olivetti G, Capasso JM. Hypertensive cardiomyopathy: myocyte nuclei hyperplasia in the mammalian rat heart. *J Clin Invest*. 1990;85:994–997.
20. Spillmann F, Van Linthout S, Schultheiss HP, Tschope C. Cardioprotective mechanisms of the kallikrein-kinin system in diabetic cardiopathy. *Curr Opin Nephrol Hypertens*. 2006;15:22–29.
21. Shakibaei M. Inhibition of chondrogenesis by integrin antibody in vitro. *Exp Cell Res*. 1998;240:95–106.
22. Kruger AL, Peterson S, Turkseven S, Kaminski PM, Zhang FF, Quan S, Wolin MS, Abraham NG. D-4F induces heme oxygenase-1 and extracellular superoxide dismutase, decreases endothelial cell sloughing, and improves vascular reactivity in rat model of diabetes. *Circulation*. 2005;111:3126–3134.
23. Oda MN, Bielicki JK, Berger T, Forte TM. Cysteine substitutions in apolipoprotein A-I primary structure modulate paraoxonase activity. *Biochemistry*. 2001;40:1710–1718.
24. Hyka N, Dayer JM, Modoux C, Kohno T, Edwards CK 3rd, Roux-Lombard P, Burger D. Apolipoprotein A-I inhibits the production of interleukin-1beta and tumor necrosis factor-alpha by blocking contact-mediated activation of monocytes by T lymphocytes. *Blood*. 2001;97:2381–2389.
25. Zou MH, Shi C, Cohen RA. High glucose via peroxynitrite causes tyrosine nitration and inactivation of prostacyclin synthase that is associated with thromboxane/prostaglandin H(2) receptor-mediated apoptosis and adhesion molecule expression in cultured human aortic endothelial cells. *Diabetes*. 2002;51:198–203.
26. Condorelli G, Morisco C, Stassi G, Notte A, Farina F, Sgaramella G, de Rienzo A, Roncarati R, Trimarco B, Lembo G. Increased cardiomyocyte apoptosis and changes in proapoptotic and antiapoptotic genes bax and bcl-2 during left ventricular adaptations to chronic pressure overload in the rat. *Circulation*. 1999;99:3071–3078.
27. Uchiyama T, Engelman RM, Maulik N, Das DK. Role of Akt signaling in mitochondrial survival pathway triggered by hypoxic preconditioning. *Circulation*. 2004;109:3042–3049.
28. Webster KA. Aktion in the nucleus. *Circ Res*. 2004;94:856–859.
29. Nishikawa T, Edelstein D, Du XL, Yamagishi S, Matsumura T, Kaneda Y, Yorek MA, Beebe D, Oates PJ, Hammes HP, Giardino I, Brownlee M. Normalizing mitochondrial superoxide production blocks three pathways of hyperglycaemic damage. *Nature*. 2000;404:787–790.
30. Westermann D, Rutschow S, Van Linthout S, Linderer A, Bucker-Gartner C, Sobirey M, Riad A, Pauschinger M, Schultheiss HP, Tschope C. Inhibition of p38 mitogen-activated protein kinase attenuates left ventricular dysfunction by mediating pro-inflammatory cardiac cytokine levels in a mouse model of diabetes mellitus. *Diabetologia*. 2006;49:2507–2513.
31. Dewald O, Frangogiannis NG, Zoerlein M, Duerr GD, Klemm C, Knuefermann P, Taffet G, Michael LH, Crapo JD, Welz A, Entman ML. Development of murine ischemic cardiomyopathy is associated with a transient inflammatory reaction and depends on reactive oxygen species. *Proc Natl Acad Sci U S A*. 2003;100:2700–2705.
32. Shen X, Zheng S, Metreveli NS, Epstein PN. Protection of cardiac mitochondria by overexpression of MnSOD reduces diabetic cardiomyopathy. *Diabetes*. 2006;55:798–805.

33. Suzuki K, Murtuza B, Sammut IA, Latif N, Jayakumar J, Smolenski RT, Kaneda Y, Sawa Y, Matsuda H, Yacoub MH. Heat shock protein 72 enhances manganese superoxide dismutase activity during myocardial ischemia-reperfusion injury, associated with mitochondrial protection and apoptosis reduction. *Circulation*. 2002;106(suppl I):I-270–I-276.
34. Frustaci A, Kajstura J, Chimenti C, Jakoniuk I, Leri A, Maseri A, Nadal-Ginard B, Anversa P. Myocardial cell death in human diabetes. *Circ Res*. 2000;87:1123–1132.
35. Lakhani SA, Masud A, Kuida K, Porter GA Jr, Booth CJ, Mehal WZ, Inayat I, Flavell RA. Caspases 3 and 7: key mediators of mitochondrial events of apoptosis. *Science*. 2006;311:847–851.
36. Susin SA, Zamzami N, Castedo M, Hirsch T, Marchetti P, Macho A, Daugas E, Geuskens M, Kroemer G. Bcl-2 inhibits the mitochondrial release of an apoptogenic protease. *J Exp Med*. 1996;184:1331–1341.
37. Song L, De Sarno P, Jope RS. Central role of glycogen synthase kinase-3beta in endoplasmic reticulum stress-induced caspase-3 activation. *J Biol Chem*. 2002;277:44701–44708.

CLINICAL PERSPECTIVE

The present study reports that an increase in high-density lipoprotein (HDL) via human apolipoprotein A-I gene transfer reduces the development of experimental diabetic cardiomyopathy. Besides the demonstration of cardiac antiinflammatory, antioxidative, and antiapoptotic features of HDL, the present study describes new cardioprotective effects of HDL. It shows for the first time that fibrosis and glycogen accumulation are reduced after human apolipoprotein A-I transfer in an experimental model of diabetic cardiomyopathy. This study, performed in an animal model characterized by severe hyperglycemia, oxidative stress, and a ratio of HDL cholesterol to low-density lipoprotein cholesterol of 1, strongly suggests that HDL has direct cardioprotective effects, which is strengthened by the finding that HDL directly improves impaired cardiomyocyte contractility ex vivo. Our findings underscore the cardioprotective effects of HDL; however, the relevance of the use of HDL-raising therapies for the cotreatment of diabetic cardiomyopathy should be examined in future studies investigating the effect of increasing HDL on established diabetic cardiomyopathy. Moreover, it has to taken into account that the current HDL-elevating drugs only moderately increase HDL compared with apolipoprotein A-I gene transfer. Furthermore, the way that these drugs interfere with HDL metabolism differs, which might contribute to important differences in success and tolerability.